Tropical Medicine and Infectious Disease

MDPI

Article

Ecological Niche and Epidemic Risk Mapping of Lyme Disease Spirochete in Inner Mongolia, China

Dan Liu [1,†], Jiamin Yin [1,†], Yu Wang [1], Yu Zhang [1], Junliang Zhao [1], Xin Li [1], Yingjie Wang [1], Haiping Wang [2], Temure [3], Haicheng Liu [3], Ruijun Liu [4], Rui Zhang [4], Xia Wang [4], Wulantuya [1,*] and Gaowa [1,*]

[1] Inner Mongolia Key Laboratory of Vector-Borne Zoonotic Infectious Diseases, Hetao College, Bayannur 015000, China; liudan_summer@163.com (D.L.); yinjiamin5807@163.com (J.Y.); viosi.9200@foxmail.com (Y.W.)
[2] Bayannur Animal Husbandry Service Center, Bayannur 015000, China; bynrwhp@126.com
[3] Bayannur Animal Disease Prevention and Control Center, Bayannur 015000, China; 13304785776@163.com (H.L.)
[4] Linhe District Animal Disease Prevention and Control Center, Bayannur 015000, China; lrj6059@163.com (R.L.); 15047276470@163.com (R.Z.); wx-0478@163.com (X.W.)
* Correspondence: wlty-1971@163.com (W.); melody_gaowa@163.com (G.)
† These authors contributed equally to this work.

Abstract

(1) Background: Lyme disease spirochetes are obligate tick-borne pathogens causing zoonotic natural focal diseases in humans and animals. Their regional epidemic prevalence relies heavily on the distribution and population dynamics of vector ticks and reservoir hosts, posing potential public health risks in Inner Mongolia. Clarifying the spatial distribution, key driving factors, and epidemic risks of Lyme disease spirochetes is critical for targeted regional tick-borne disease prevention. Systematic mapping of suitable habitats, key environmental drivers, and epidemic risks is urgently needed for targeted prevention. (2) Methods: By integrating 2015–2026 field sampling data, published literature records, and multi-source environmental and climatic datasets, we applied an optimized MaxEnt model to simulate suitable habitats of Lyme disease spirochetes across Inner Mongolia. We analyzed core environmental drivers, projected habitat shifts under the 2050s climate scenario, characterized regional differentiation and complementary distribution of dominant vector ticks, and conducted a comprehensive spatial risk assessment to delineate Lyme disease epidemic risk zones. (3) Results: Suitable habitats exhibited marked spatial aggregation, with high-suitability areas concentrated in the eastern Greater Khingan Mountains and northern mountainous regions of Inner Mongolia, whereas western desert and Gobi areas were unsuitable for survival. Under the 2050s climate scenario, suitable habitats will expand westward with elevated overall suitability. Precipitation of the wettest quarter (Bio16) and annual mean temperature (Bio1) were the dominant driving factors, with a cumulative contribution of 64.0%, and their optimal adaptive thresholds were quantified. High-risk areas were mainly distributed in Hulunbuir, Hinggan League, and Xilingol League, with scattered high-risk sites in northern Bayannur, while western regions, including Alxa, were classified as low risk. (4) Conclusions: This study systematically elucidates the spatial distribution, climatic driving mechanisms, and epidemic risk differentiation of Lyme disease spirochetes and their dominant vectors in Inner Mongolia, providing scientific support for precise local Lyme disease control and a theoretical basis for formulating targeted tick-borne disease prevention strategies in northern China's grassland ecosystems.

Keywords: Lyme disease spirochete; risk assessment; climate driving factors; Inner Mongolia

Check for updates

Academic Editor: John Frean

Received: 20 October 2026
Revised: 20 November 2026
Accepted: 25 November 2026
Published: 29 November 2026

Copyright: © 2026 by the authors. Licensee MDPI, Basel, Switzerland. This article is an open access article distributed under the terms and conditions of the Creative Commons Attribution (CC BY) license.

1. Introduction

Borrelia spirochetes are divided into Lyme disease spirochetes and relapsing fever borreliae. Lyme disease spirochete are tick-borne pathogens that cause Lyme disease, with ticks serving as their primary transmission vectors [1,2]. Since *Borrelia burgdorferi* was identified as the etiological agent of Lyme disease in 1981 [3], multiple genospecies, including *B. burgdorferi* sensu stricto, *B. garinii*, *B. afzelii*, *B. bavariensis,* and *B. spielmanii,* have been reported worldwide, with distinct differences in geographical distribution and associated clinical manifestations [4–6]. The first human case of Lyme disease in China was diagnosed in Heilongjiang Province in 1985 [7]. To date, seropositive individuals have been detected across over 30 provincial-level administrative regions [8–10]. At least five genotypes circulate in China, among which *B. garinii* and *B. afzelii* are the dominant pathogenic genospecies [10]. Human infection occurs via bites of infected ticks. The pathogen can invade the skin, joints, nervous system, and cardiovascular system, and delayed treatment frequently leads to persistent chronic lesions [11]. Accordingly, Lyme disease has become a major public health concern in Europe, North America, as well as forest areas of Northeast China [9–11].

Globally, all well-documented competent vectors of Lyme disease spirochetes belong to the genus *Ixodes* [12,13]. The principal vector species include *I. scapularis* in eastern North America, *I. pacificus* on the North American Pacific coast, *I. ricinus* throughout Europe, and *I. persulcatus* across eastern Eurasia [1,11,12]. Small rodent mammals serve as the core reservoir hosts sustaining the enzootic cycle of the *B. burgdorferi* sensu lato complex. In North America, *Peromyscus leucopus* is the dominant reservoir host; in Europe, *Clethrionomys glareolus*, *Apodemus sylvaticus*, and *A. flavicollis* maintain pathogen circulation; and forest ecosystems of East Asia rely primarily on *A. peninsulae*, *C. rufocanus*, and *A. agrarius* as reservoir hosts [1,14,15]. These canonical vectors and rodent hosts exhibit striking spatial differentiation across Inner Mongolia. The forested zone of the Greater Khingan Mountains in eastern Inner Mongolia supports stable populations of *I. persulcatus*, together with typical forest rodent reservoirs including *A. peninsulae* and *C. rufocanus* [16–19], forming a well-characterized forest-type natural focus of Lyme disease in China. Although competent tick vectors of Lyme disease spirochetes belonging to the genus *Ixodes* are absent in central and western Inner Mongolia, pathogenic *B. garinii* and *B. afzelii* have been successfully amplified from samples of *Dermacentor nuttalli*, *Hyalomma asiaticum*, and desert rodents (*Meriones unguiculatus* and *Phodopus sungorus*) collected in grassland areas of central and western Inner Mongolia in multiple molecular epidemiological surveys [20–22]. These findings strongly suggest local enzootic circulation of Lyme disease spirochetes within this distinctive steppe ecosystem.

The spatial distribution and health impacts of Lyme disease are governed by three key components: pathogens, tick vectors, and animal reservoir hosts. Its transmission cycle is constantly affected by human activities, climate change, and land use alteration [19,23]. Over the past two decades, tick populations in temperate regions have expanded northward and to higher altitudes, mainly driven by rising temperatures and prolonged activity periods [24–26]. These environmental changes not only facilitate tick development and host-seeking behavior but also alter temperature and humidity conditions to indirectly influence the survival and proliferation of the Lyme disease spirochete [25,27]. Furthermore, urban expansion has reduced natural habitats. Combined with climate change and suburban forest fragmentation, the frequency of human-tick contact has increased remarkably, resulting in sustained high incidence of Lyme disease in some local areas [23,27,28].

Inner Mongolia features vast grasslands, prosperous animal husbandry, and abundant wild rodents. Such environments support dense tick populations and the sustained circulation of the Lyme disease spirochete, putting local residents at high risk of tick ex-

posure [16,29]. To date, most regional studies have focused on cross-sectional pathogen detection and PCR screening in ticks. Comprehensive modeling that predicts spirochete habitat suitability, identifies limiting climatic factors, compares spatial patterns with dominant tick vectors, and forecasts future risk under climate change remains lacking. The primary objectives of this study were to: (1) simulate the current suitable habitat of Lyme disease spirochetes across Inner Mongolia using an optimized MaxEnt model; (2) quantify key environmental predictors shaping spirochete distribution and estimate range changes under the 2050s climate scenario; (3) examine spatial associations between spirochete suitable habitats and the distribution of dominant tick vectors; and (4) map regional epidemic risk zones to inform surveillance priorities. This work fills the above research gap and provides actionable evidence for Lyme borreliosis surveillance and risk-based prevention in northern China grasslands.

2. Materials and Methods

2.1. Compilation of Geospatial Occurrence Data

In order to acquire credible distribution records of target pathogens and tick vectors, this research integrated field sampling datasets gathered from 2015 to 2026 and geospatial information extracted from existing published studies. We primarily sorted out coordinate data of sites where Lyme disease spirochetes were positively detected (Supplementary Table S1), as well as occurrence records of four dominant tick transmission vectors, namely *Dermacentor nuttalli*, *Haemaphysalis concinna*, *Hyalomma asiaticum*, and *Ixodes persulcatus*. All geocoordinate records were entered into Excel spreadsheets, followed by import into ArcMap 10.2 (Esri, Redlands, CA, USA) for spatial preprocessing. The datasets were then transformed into Shapefile vector layers, with unified spatial normalization and calibration conducted based on the WGS1984 geodetic coordinate system. Repeated sampling records easily lead to data redundancy and further raise the risk of model overfitting. Taking the pixel size of environmental covariate layers as the spatial filtering criterion, we adopted ENMtools (Warren, D.L., University of California, Davis, CA, USA) to delete redundant overlapping distribution points within a single grid unit.

2.2. Laboratory Detection of Lyme Disease Spirochetes

Tick specimens were collected across multiple sampling sites in Inner Mongolia from 2015 to 2026. Field surveys were carried out during the active season of ticks (April to September). Ticks were collected by flagging vegetation with white flannel cloth and by examining domestic animals (cattle, sheep, and horses). Tick species identification was performed by morphological characteristics [30] and mitochondrial 16S rDNA (mt-rrs) gene sequencing [31].

Genomic DNA was extracted individually from each tick specimen subjected to pathogen screening. A subset of the collected ticks was tested for Lyme disease spirochetes, comprising 1922 *D. nuttalli*, 570 *Hae. concinna*, and 354 *Hy. asiaticum*. The PCR-positive rates were 3.4% (66/1922) for *D. nuttalli*, 6.7% (38/570) for H. concinna, and 2.5% (9/354) for *Hy. asiaticum*. Target fragments of the *flaB* (flagellin) gene of Lyme disease spirochetes were amplified by conventional PCR following the protocol reported by [32]. The thermal cycling program included an initial predenaturation step, followed by 30 cycles of 95 °C for 30 s (denaturation), 50 °C for 30 s (annealing), and 72 °C for 60 s (extension). Positive and negative controls were included in every PCR batch to assess amplification reliability and rule out contamination. Amplicons were separated via agarose gel electrophoresis, and fragments of the expected size were purified and subjected to Sanger sequencing for genospecies confirmation.

2.3. Screening and Preprocessing of Bioclimatic Environmental Variables

2.3.1. Collection of Multi-Source Environmental Datasets

Multiple types of environmental data from authoritative open-access databases were compiled in this research to support follow-up analyses. Nineteen bioclimatic predictors together with elevation information were downloaded from the WorldClim database at a uniform spatial resolution of 2.5 arc-minutes. Livestock density records were acquired via the official database maintained by the Food and Agriculture Organization of the United Nations (FAO). Soil pH and soil organic carbon datasets came from the National Earth System Science Data Center, while the Resource and Environmental Science Data Center provided Normalized Difference Vegetation Index (NDVI), population density, GDP, and land-use classification data. Furthermore, digital elevation models were imported into the spatial analysis toolkit of ArcMap to generate terrain parameters such as slope and aspect. Full descriptions of all environmental predictors are presented in Supplementary Table S2. The administrative boundary of Inner Mongolia was designated as the research extent. Using core functions within ArcGIS 10.2, namely resampling, mask extraction, and raster projection conversion, environmental raster layers corresponding to the study region were extracted. Uniform geographic coordinate systems and pixel dimensions were implemented for all raster layers. Preprocessed environmental datasets were exported as ASC files, forming the basic input dataset for constructing the MaxEnt (Phillips, S.J., Princeton University, Princeton, NJ, USA) species distribution model.

2.3.2. Pre-Selection and Collinearity Removal of Environmental Predictors

Collinearity among environmental predictors may impair model performance, potentially leading to overfitting and decreased predictive accuracy [33,34]. We began with 29 initial predictors and ran preliminary MaxEnt simulations with Lyme disease spirochete occurrence records. Records were partitioned into 75% training and 25% test data under default settings. Jackknife tests and 10 bootstrap replicates with 10,000 background points and 500 model iterations were used to assess variable contributions. Variables with zero contribution were discarded, leaving 11 candidates. Spearman correlation analysis ($|r| \geq 0.8$) was then performed on these 11 variables in R (ggplot package) to remove highly collinear predictors. Eventually, 6 low-collinearity optimal predictors were retained for formal MaxEnt modeling, including precipitation of wettest quarter (Bio 16), annual mean temperature (Bio 1), precipitation of wettest month (Bio 13), Normalized Difference Vegetation Index (NDVI), slope aspect (Asp), and isothermality (Bio 3).

2.4. Optimization and Accuracy Validation of the MaxEnt Model

The predictive capacity of the MaxEnt model is governed by two key parameters: feature classes (FC) and regularization multiplier (RM). These parameters exert direct influences on model overfitting risk and predictive stability [35]. To boost model predictive performance, the ENMeval package in R (v3.6.1) was adopted to identify the optimal FC and RM combination. Models with default settings (RM = 1, FC = LQHPT) were taken as the reference group. Five feature class types were considered: linear (L), quadratic (Q), product (P), threshold (T), and hinge (H). The regularization multiplier varied from 0.5 to 4 with 0.5 increments, generating 256 distinct parameter combinations in total. Comprehensive screening for the optimal model was conducted relying on three metrics: delta-corrected Akaike information criterion (delta AICc), the area under the ROC curve (AUC), and 5% training omission rate (OR_5) [36]. The collinearity-filtered environmental variables and occurrence records of Lyme disease spirochete were loaded into the optimized MaxEnt model with the selected FC and RM values, while other modeling configurations were kept consistent. Model predictive performance was assessed via ROC curves and corresponding

AUC values, which range between 0 and 1. According to widely adopted criteria: AUC < 0.7 indicates poor predictive power; 0.7–0.8 indicates moderate power; 0.8–0.9 indicates good power; and 0.9–1.0 indicates excellent power.

2.5. Current and Future Distribution Pattern of Lyme Disease Spirochete

The MaxEnt model outputs continuous habitat suitability indices ranging from 0 to 1, where 0 indicates entirely unsuitable habitats, and 1 represents highly suitable habitats. ASCII files exported from the model were imported into ArcMap 10.2 and converted to raster datasets. After optimizing the display symbology, the Jenks natural breaks classification method was adopted to classify the potential suitable habitats of Lyme disease spirochete into four levels: unsuitable, low suitability, moderate suitability, and high suitability, to reveal the spatial distribution characteristics of habitats with different suitability. Future climate data were obtained from the BCC-CSM2-MR global climate model under the CMIP6 framework. Future climatic datasets for the 2050s (average period 2041–2060) were obtained from two CMIP6 global climate models, BCC-CSM2-MR and EC-Earth3-Veg. Four representative shared socioeconomic pathways (SSPs) covering a gradient of emission levels were selected to quantify prediction uncertainty: SSP1-2.6 (low-emission sustainable pathway), SSP2-4.5 (intermediate emission pathway), SSP3-7.0 (moderately high emission pathway), and SSP5-8.5 (high-emission fossil-fuel-intensive pathway). Projections from the two GCMs were used to assess climate-model-related uncertainty, while cross-scenario comparisons captured emission-pathway uncertainty.

2.6. Construction of Occurrence, Transmission, and Comprehensive Risk Prediction Models for Lyme Disease Spirochete

Taking the climatic suitability of Lyme disease spirochete, spatial distribution of dominant vector ticks, and animal host distribution as core indicators, this study established an occurrence risk evaluation system via spatial overlay analysis (Supplementary Figure S1). Furthermore, an analytic hierarchy process (AHP)-based [37] transmission risk model was developed by integrating multiple driving factors, including climatic adaptability, vector and host distribution, as well as regional traffic and trade conditions (Supplementary Figure S2). Factor weights were quantified (Supplementary Tables S3–S5) to identify potential high-transmission zones and generate spatial transmission risk maps. All occurrence and transmission suitability outputs were classified into low, moderate, and high risk levels using the Jenks natural breaks method. Taking pathogen occurrence risk as the dominant constraint, the two graded risk layers were spatially coupled, reflecting regional pathogen colonization capacity and vector-mediated cross-regional diffusion potential. Finally, a comprehensive risk zoning map for Lyme disease spirochete in Inner Mongolia was produced. According to the pairwise combination of occurrence and transmission grades, nine integrated risk types were defined, and their spatial differentiation characteristics were systematically analyzed.

3. Results

3.1. Niche Modeling and Distribution Prediction of Lyme Disease Spirochetes

3.1.1. Model Optimization and Accuracy Evaluation

The MaxEnt model was employed to predict the suitable habitats for Lyme disease spirochetes under current and future climate scenarios, using 64 confirmed occurrence records and 6 screened environmental variables. Compared with the default parameter settings, the optimized model adopted feature combination LPT and a regularization multiplier of 2 (with delta. AICc = 0). As shown in Table 1, the optimized MaxEnt model exhibited

improved performance: the mean AUC value increased from 0.781 to 0.817 (Figure 1a), and the ΔAICc value decreased from 811.014 to 0, demonstrating a robust predictive performance. Additionally, the omission rate of the test samples closely aligned with the predicted omission rate curve (Figure 1b), indicating the absence of spatial autocorrelation in the modeling dataset and a reliable simulation effect. Collectively, the comprehensive evaluation based on AUC values and omission rates confirms that the model predictions achieve high accuracy and reliability.

Table 1. Evaluation of optimization results of r-package ENMeval.

Parameter Settings	Regularization Multiplier, RM	Feature Combination, FC	Avg. Diff. AUC	delta_AICc	Mean. OR_5
Default	1	LQHP	0.781	811.014	0.15
Optimized	2	LPT	0.817	0	0

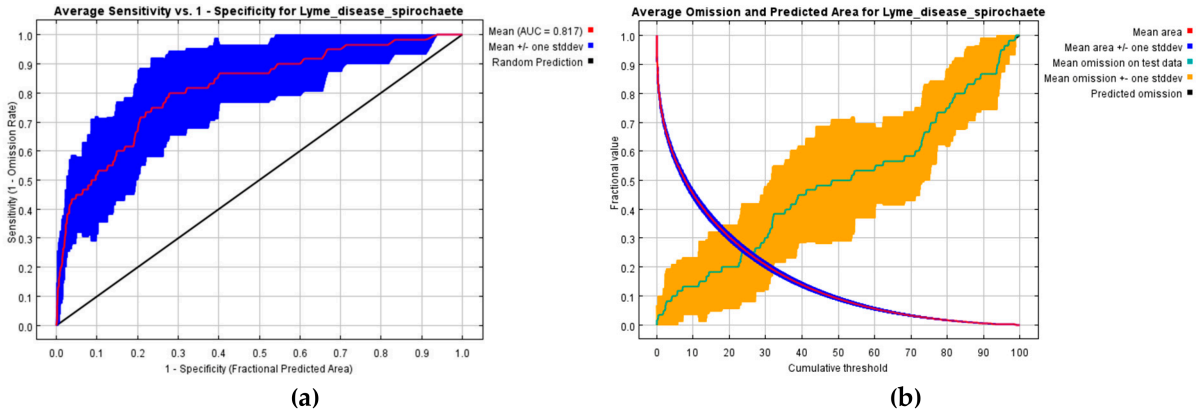
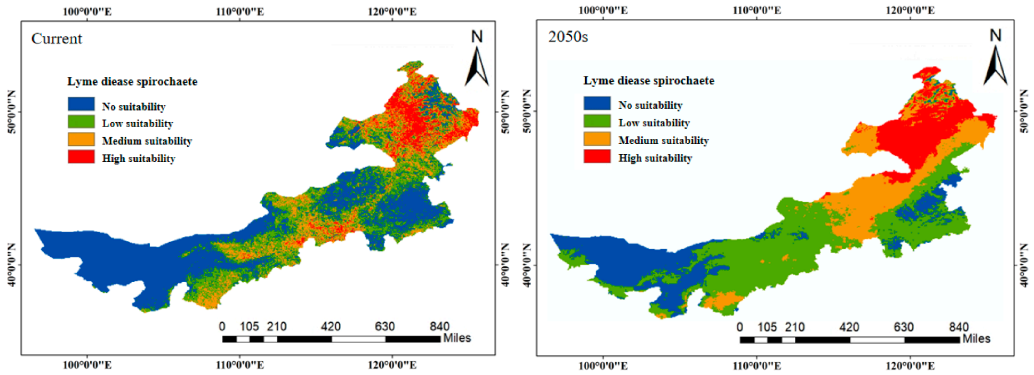


Figure 1. Model prediction accuracy analysis. (**a**) Average omission and predicted area curve. (**b**) Receiver operating characteristic (ROC) curve.

3.1.2. Current and Future Distribution Pattern of Lyme Disease Spirochetes

For the current distribution (Figure 2a), the suitable habitats of Lyme disease spirochetes in Inner Mongolia show prominent spatial clustering characteristics. High-suitability areas are concentrated in the forest-steppe ecotone and northern mountainous regions of the Greater Khingan in eastern Inner Mongolia (parts of Hulunbuir, Hinggan, and Tongliao). Medium-suitability areas are distributed in transitional zones between high- and low-suitability areas, including Xilingol and the Horqin Grassland in central Inner Mongolia. Low-suitability areas are sporadically distributed in the central typical steppe and parts of the southern Ordos Plateau. The entire desert and Gobi regions in western Inner Mongolia (Alxa and Bayannur) are unsuitable habitats.

Under the 2050s climate scenario (Figure 2b), the suitable habitats of Lyme disease spirochetes present an obvious westward expansion and suitability upgrading trend. High-suitability areas extend westward into the central grasslands of Xilingol and reach the edge of the Ordos. Medium-suitability areas largely replace the original low-suitability areas in central and southern Inner Mongolia, with an obvious expansion of the overall suitable range. The projections under SSP2-4.5 from EC-Earth3-Veg and the other three SSP scenarios (SSP1-2.6, SSP3-7.0, and SSP5-8.5) from BCC-CSM2-MR are shown in Supplementary Figure S3. Overall, the spatial patterns of suitable habitats were broadly concordant between the two GCMs across contrasting emission scenarios.



(**a**) (**b**)

Figure 2. Current and future distribution pattern of Lyme disease spirochetes. (**a**) Current climate conditions. (**b**) 2050s of BCC-CSM2-MR.

3.1.3. Identification of Key Driving Factors

The Jackknife method, contribution rate analysis, and permutation importance test were adopted to identify the key environmental driving factors affecting the suitable habitat distribution of Lyme disease spirochetes in Inner Mongolia. The threshold of suitable survival intervals was accurately determined based on the response curves, with a species presence probability greater than 0.5 defined as the suitable survival condition.

As shown in Table 2, precipitation of the wettest quarter (Bio16) was the primary dominant driving factor affecting the spatial distribution of Lyme disease spirochetes, with a contribution rate of 34.3% and a permutation importance of 55.5%. Annual average temperature (Bio1) ranked second, with a contribution rate of 29.7% and a permutation importance of 18.1%. The two core climatic factors contributed a total of 64.0%, which played a decisive role in the distribution pattern of Lyme disease spirochetes. The importance of other environmental factors followed the order: precipitation of the wettest month (Bio13, 11.6%), Normalized Difference Vegetation Index (NDVI, 10.7%), slope aspect (Asp, 8.7%), and isothermality (Bio3, 5.0%).

Table 2. Contribution rate and importance of main environmental variables..

Variable	Explanation	Percent Contribution (%)	Permutation Importance (%)
Bio16	Precipitation of wettest quarter (mm)	34.3	55.5
Bio1	Annual average temperature (°C)	29.7	18.1
Bio13	Precipitation of wettest month (mm)	11.6	1.1
NDVI	Normalized Difference Vegetation Index	10.7	13.2
Asp	Geographical orientation of slope aspect	8.7	9.8
Bio3	Isothermality (Bio 2 ÷ Bio 7 × 100) (%)	5.0	2.2

The Jackknife test results indicated that the regularization training gain of the model decreased significantly after removing Bio16 and Bio1 (Figure 3a), which further verified that precipitation and temperature were the core driving factors for the distribution of Lyme disease spirochetes. Response curve threshold analysis showed that the optimal survival temperature range was −5.3 °C to 1.8 °C (presence probability > 0.5), with the peak presence probability occurring at −4.1 °C (Figure 3b). For precipitation, the presence probability remained above 0.5 when the precipitation of the wettest quarter was above 180 mm, reached the maximum value at 340 mm, and decreased slightly when precipitation exceeded 340 mm (Figure 3c).

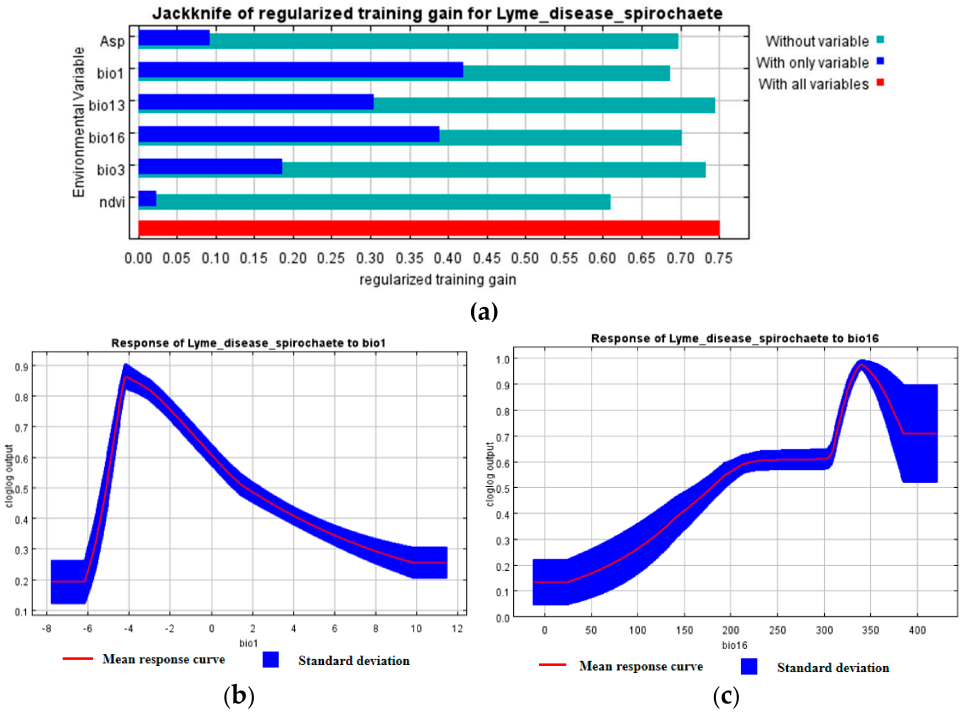


Figure 3. Identification of key driving factors. (**a**) Jackknife test for a single environmental variable. (**b**) Response curve of Bio 1. (**c**) Response curve of Bio 16.

3.2. Spatial Distribution of Lyme Disease Spirochete Vectors

The Maxent model was adopted to simulate and analyze the potential suitable habitat distribution of four main vector ticks of Lyme disease spirochetes in Inner Mongolia (Figure 4). Significant regional differentiation characteristics were observed in the spatial distribution patterns of these four tick species. *D. nuttalli* holds the widest suitable habitat coverage in Inner Mongolia and presents a continuous east-west zonal distribution. Its high-suitability areas are concentrated in the central Xilingol Grassland, southern Ordos Plateau, and eastern transitional areas, while only the western Alxa Desert and Gobi regions are entirely unsuitable habitats (Figure 4a). *I. persulcatus* habitats are highly concentrated in the Great Khingan Mountain forest areas in northeastern Inner Mongolia. Its high-suitability areas are distributed only in the northeasternmost mountain regions, and the entire central and western regions of Inner Mongolia are unsuitable habitats (Figure 4b). The distribution pattern of *Hae. concinna* is highly similar to that of *I. persulcatus*. Its suitable habitats are concentrated in the Great Khingan Mountains and surrounding forest-steppe areas in eastern Inner Mongolia, with high-suitability areas in the northeastern mountains, and most central and western regions are unsuitable habitats (Figure 4c). *Hy. asiaticum* presents an east-west zonal distribution along southern and southwestern Inner Mongolia. Its high-suitability areas are concentrated in the western desert steppe, while the Ordos Plateau and the entire northeastern forest areas are unsuitable habitats (Figure 4d).

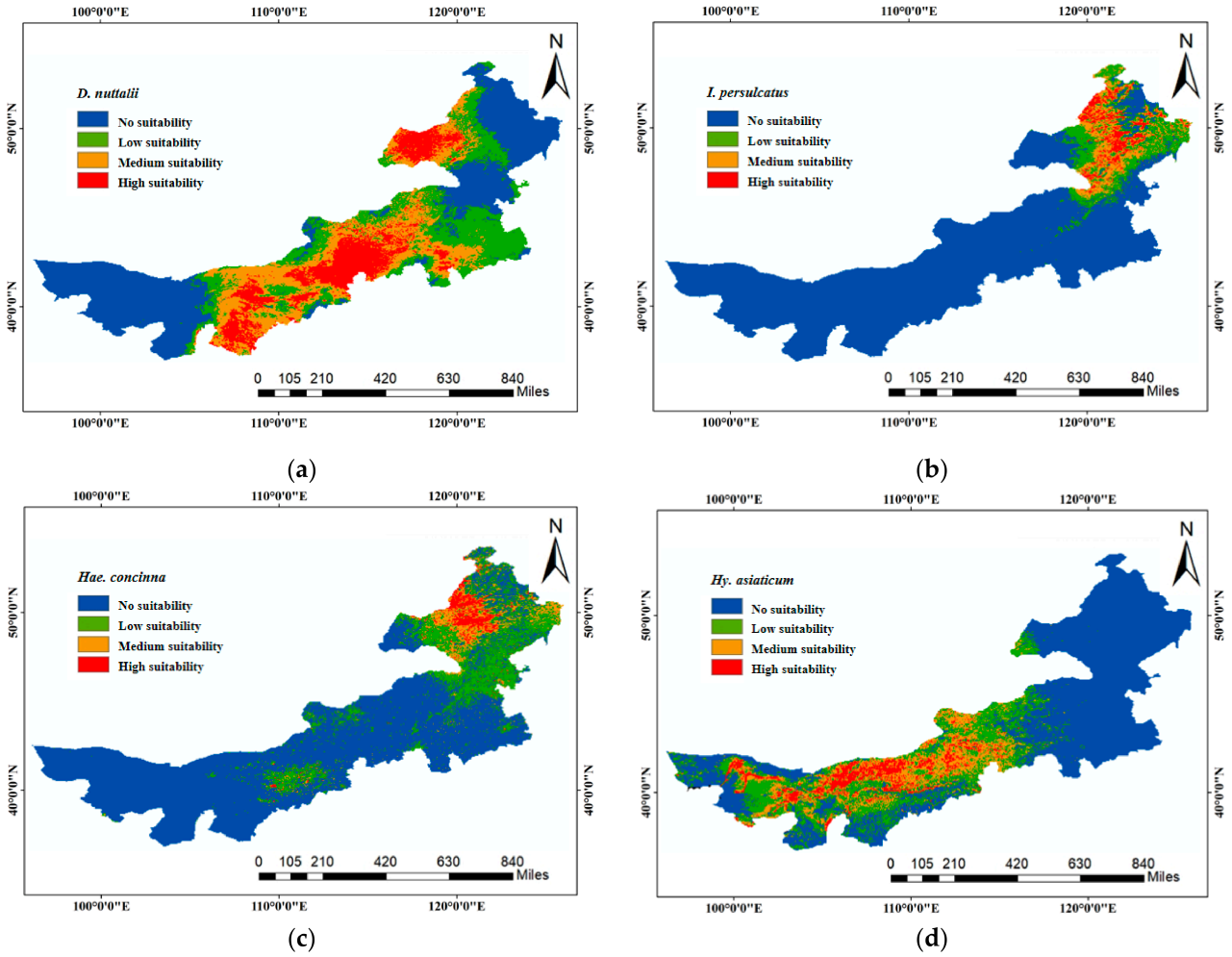


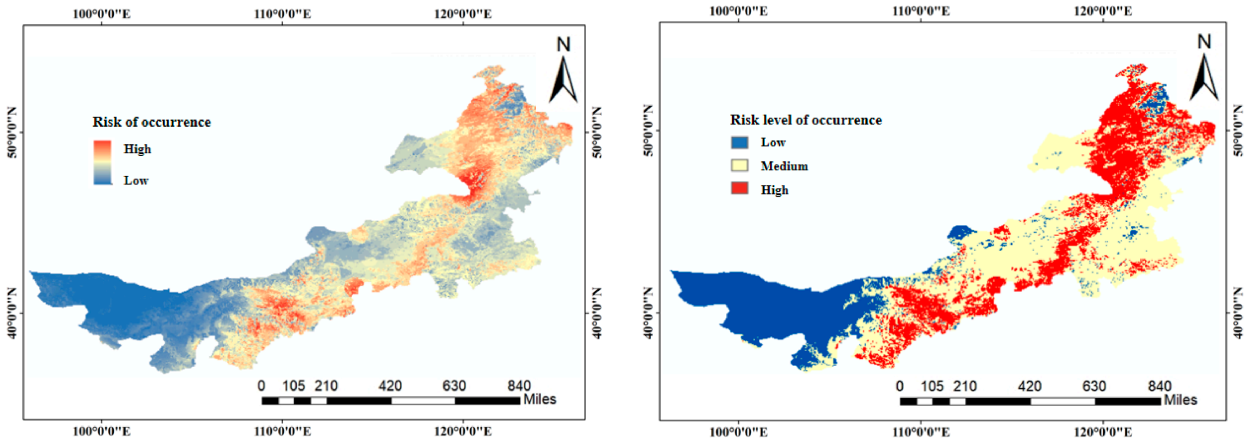
Figure 4. Distribution of the main vectors for Lyme disease spirochetes. (**a**) *D. nuttalli*. (**b**) *I. persulcatus*. (**c**) *Hae. concinna*. (**d**) *Hy. asiaticum*.

The suitable habitats of the four tick species show an obvious east-west complementary spatial differentiation rule. The dominant vector ticks in the northeastern mountain forest areas of Inner Mongolia are *I. persulcatus* and *Hae. concinna*. The dominant vector tick in central grassland areas and southern plateau areas is *D. nuttalli*, and the dominant vector tick in the western desert steppe is *H. asiaticum*.

3.3. Construction of a Risk Prediction Model for Lyme Disease Spirochetes

3.3.1. Occurrence Risk Analysis

The spatial overlay of climate suitability of Lyme disease spirochetes, the comprehensive distribution of vector ticks, and the distribution of animal hosts was conducted to construct an occurrence risk assessment model for Lyme disease spirochetes. Figure 5a shows that the occurrence suitability of Lyme disease spirochetes presents an overall spatial gradient of low in the west and high in the east. Highly suitable areas are concentrated in the central Xilingol Grassland, northern Ulanqab, and northwestern Chifeng of Inner Mongolia, while the western Alxa Desert regions and eastern Greater Khingan forest areas show relatively low suitability.



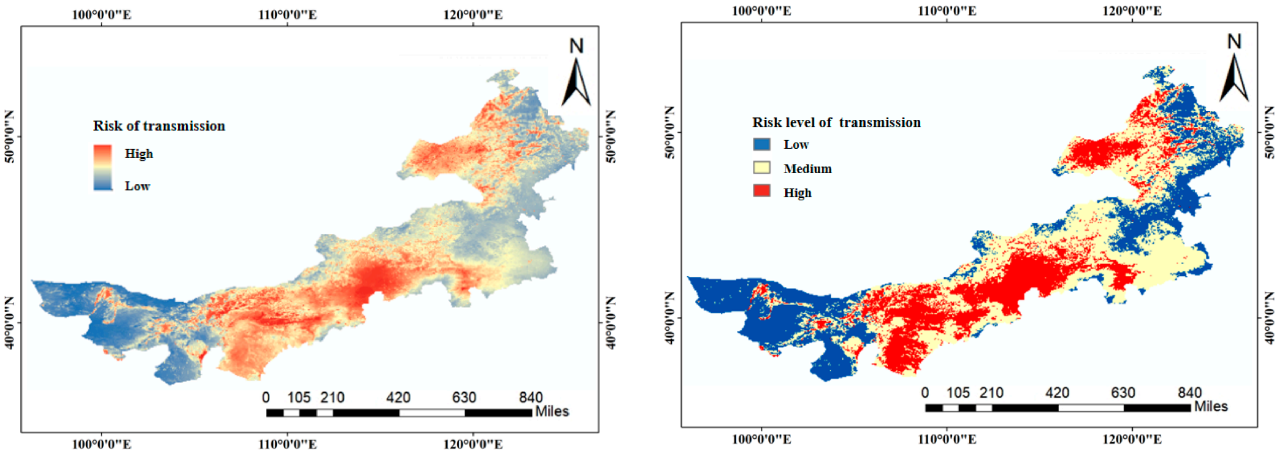
(**a**) (**b**)

Figure 5. Occurrence risk analysis for Lyme disease spirochetes. (**a**) Continuous occurrence risk. (**b**) Occurrence risk classified by the natural breakpoint method.

The Jenks natural breaks classification method was adopted to divide occurrence suitability into three risk levels: low, medium, and high. The graded risk spatial distribution map (Figure 5b) indicates that high occurrence risk areas are continuously concentrated in the central and eastern grasslands of Inner Mongolia. Medium-risk areas form a transitional surrounding pattern, and the entire western Alxa and northern Greater Khingan forest areas in the northeast are stable low-risk regions.

3.3.2. Spread Risk Analysis

Based on AHP, multiple factors, including traffic and trade exchanges, distribution of vector ticks, and animal hosts, were comprehensively integrated to identify potential high-risk areas for the transmission and spread of Lyme disease spirochetes and complete risk mapping. Figure 6a shows that the regional transmission potential is generally consistent with the occurrence suitability pattern. The central and southern grasslands show significantly high transmission suitability, while the western desert and northeastern forest areas have poor transmission conditions.



(**a**) (**b**)

Figure 6. Transmission risk analysis for Lyme disease spirochetes. (**a**) Continuous transmission risk. (**b**) Transmission risk classified by the natural breakpoint method.

The Jenks natural breaks classification method was also used for transmission risk grading. The graded risk map (Figure 6b) reveals that high-transmission-risk areas are continuously zonally distributed in south-central Inner Mongolia, covering southern Xilingol, southern Ulanqab, the Ordos Plateau, and western Chifeng. Medium-risk areas gradually shrink outward, and western Alxa as well as northeastern mountain forest areas are all low-transmission-risk areas.

3.3.3. Comprehensive Risk Analysis

Taking the occurrence risk of Lyme disease spirochetes as the dominant factor, the occurrence risk layer and transmission risk layer were graded separately using the Jenks natural breaks classification method. Spatial overlay analysis was performed to obtain the spatial distribution map of comprehensive occurrence-transmission risk levels of Lyme disease in Inner Mongolia (Figure 7).

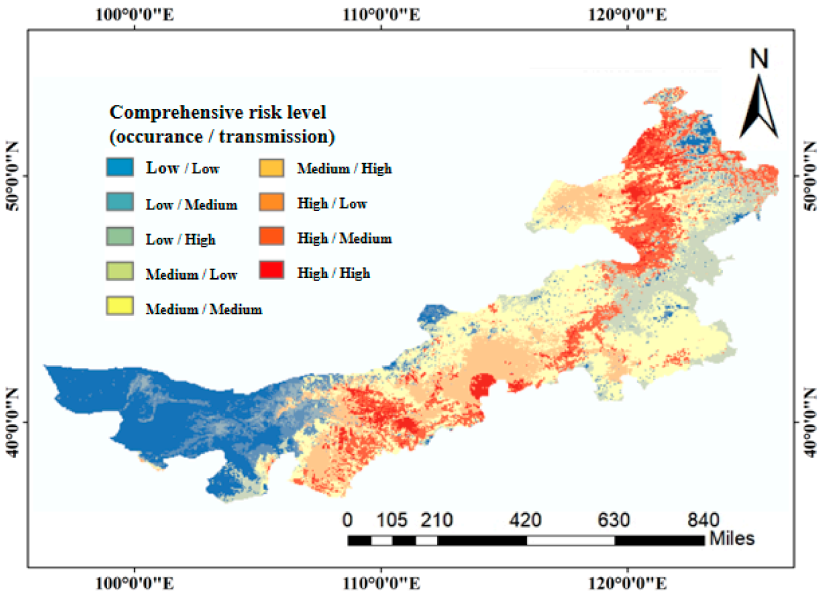


Figure 7. Comprehensive risk analysis for Lyme disease spirochetes.

The comprehensive Lyme disease risk in the study area presents distinct spatial differentiation. High-High risk areas and High-Medium comprehensive risk areas are contiguously concentrated in most parts of Hulunbuir and western Hinggan League, and are distributed in continuous strips in south-central Xilingol League. In addition, such areas are patchily scattered in northern Bayannur, eastern Ordos, and the southern mountainous areas of Baotou. Medium-High and Medium/Medium combined risk areas form annular transitional belts surrounding high-risk core zones at all levels. Low/Medium and Low/High risk areas are sporadically interspersed in the central transitional zones. Extensive continuous Low-Low comprehensive risk areas are distributed across the entire desert-Gobi region of Alxa in western Inner Mongolia.

4. Discussion

4.1. Niche Suitability of Lyme Disease Spirochetes and Climate-Driven Distribution Mechanisms

MaxEnt models were calibrated with LPT feature classes and a regularization multiplier of 2 using 64 georeferenced Lyme disease spirochete occurrence records and 6 pre-screened environmental predictors. This calibration delivered a ΔAICc value of 0, while the average AUC value increased moderately from 0.781 to 0.817. Previous studies have shown that ecological niche modeling of *B. burgdorferi* in Ontario, Canada employed LQ feature classes

with RM = 1.5 and yielded an AUC of 0.963 [38], while prediction of suitable areas for *R. japonica* in China and adjacent regions selected LQP features with RM = 1 through ENMeval optimization [39]. These findings indicate that optimal parameter combinations for pathogen MaxEnt models vary among species due to differences in environmental responses and sample sizes. The optimized model can reduce overfitting or underfitting, thereby enabling accurate identification of potential expansion areas [29,40].

Under current climatic conditions, spirochete habitat suitability generally follows the east-to-west forest–steppe–desert ecological zonation of Inner Mongolia. Regions with relatively high suitability are mostly confined to the forest-steppe ecotones of the Greater Khingan Mountains, where field surveillance has repeatedly identified tick-borne disease hotspots [41,42]. Central Xilingol and the Horqin grasslands likely function as transitional zones with moderate suitability, whereas the Gobi landscapes in western Alxa and Bayannur tend to offer few viable habitats, largely due to persistent extreme aridity that supports only limited tick populations [29]. Such spatial patterns appear consistent with field surveillance data, where low *Borrelia* positivity rates are commonly detected in tick specimens collected from western areas [16,42]. Projections for the 2050s indicate that climate warming and humidification could ease aridity-related restrictions across mid-western steppe regions. Correspondingly, zones with relatively high suitability may expand westward toward the central Xilingol grasslands and the marginal zones of the Ordos Plateau, and a considerable proportion of originally low-suitability steppe habitats may shift to moderate suitability. Comparable range shifts associated with climatic change have been reported for other Eurasian tick-borne pathogens, with tick vectors and associated *Borrelia* expanding toward higher latitudes and altitudes [43–45]. In European Russia, climatic warming has already been linked to prolonged tick activity seasons and altered borreliosis incidence dynamics across previously non-endemic zones [46]. Yet most regional investigations to date have only mapped tick vector distributions, with limited quantification of climate thresholds specific to *Borrelia* [29]. The modeled distribution shifts imply that endemic hotspots previously concentrated in northeastern mountain forests may gradually expand westward, which could challenge conventional surveillance strategies that mainly target eastern woodlands [43].

Integrated analyses suggest that precipitation of the wettest quarter (Bio16, 34.3%) and annual mean temperature (Bio1, 29.7%) are likely the primary environmental regulators. This dominance of temperature and precipitation variables aligns with broader ecological niche modeling of tick-borne systems, where thermal and hydric conditions are repeatedly identified as principal limiting factors for off-host tick survival and pathogen persistence [43,44]. Removing either variable tends to induce a notable drop in model training gain, further hinting at their vital roles. Response curves point to a potential cold-adapted trait of local *Borrelia* populations: suitable survival temperatures range roughly from −5.3 °C to 1.8 °C, with occurrence probability possibly peaking at −4.1 °C. Importantly, this temperature range reflects macroclimatic mean annual conditions across cold high-latitude and high-elevation landscapes, rather than fine-scale microclimatic temperatures that directly govern spirochete replication and seasonal activity within ticks. This preference for cool environments is consistent with previous findings that tick-borne *Borrelia* in temperate and boreal regions thrive under relatively low annual temperature conditions [47]. Sustained pathogen colonization may require wettest-quarter precipitation above 180 mm, with an apparent optimum around 340 mm, after which suitability may slightly decline under excessive rainfall. This unimodal precipitation response parallels documented thresholds for *Ixodes* ticks [47]. These quantified niche thresholds help explain the marked east–west suitability gradient and resolve a regional research gap, facilitating the construction of semi-quantitative early-warning frameworks for local disease risk.

4.2. Niche Partitioning of Primary Tick Vectors and Potential Influences on Endemic Patterns

Simultaneous niche modeling of the four dominant tick species revealed limited overlap in their core suitable habitats, forming a roughly complementary east–west zonal distribution that corresponds to the heterogeneous landscapes of Inner Mongolia and constitutes relatively independent vector-borne transmission systems. *D. nuttalli* showed the widest ecological tolerance, with high-suitability areas scattered across the central Xilingol steppes and the southern Ordos Plateau, making it the most likely primary vector in grassland and plateau ecosystems; its high haplotype diversity (0.983) in Inner Mongolia further supports its adaptability to diverse habitats [48]. *I. persulcatus* is the core vector of Lyme disease spirochetes, and the distribution of *Hae. concinna* nearly overlaps with that of *I. persulcatus* in Inner Mongolia; both species have similar niche requirements and are concentrated in the cool, humid forests of the Greater Khingan Mountains, with almost no suitable habitats in the central and western parts of the study region. *Hy. asiaticum*, in contrast, mainly occupies the western desert steppes and the Ordos Plateau, whereas the northeastern forest zones offer poor survival conditions. These distributions are consistent with the field survey results of Ma et al. [29]. Lyme disease spirochetes have been detected in all four tick species in previous studies [16]. Positive PCR results only indicate pathogen presence in collected ticks and should not be interpreted as evidence of vector competence or ongoing local transmission. Combined with their marked spatial segregation, these detection records suggest that potential natural foci may be geographically partitioned across Inner Mongolia. Based on this vector zoning pattern, targeted surveillance and control strategies should be adopted for different landscape types.

4.3. Integrated Lyme Disease Risk Assessment Combining Natural Ecological Conditions and Anthropogenic Activities

A natural occurrence risk model was constructed by integrating three layers of data, including climatic suitability for *Borrelia*, distribution of tick vectors, and ranges of reservoir hosts. This model fully characterizes the pathogen–vector–host transmission cycle and mitigates the bias of single-factor models relying merely on climatic variables, which tend to overestimate disease risk in forested areas while underestimating epidemic potential in steppe regions [1,49]. The occurrence risk of Lyme disease across Inner Mongolia exhibits an overall east-high and west-low spatial gradient. Continuous high-occurrence-risk zones are located in the central Xilingol Grassland, northern Ulanqab, and northwestern Chifeng, where habitats suitable for pathogen survival, abundant tick populations, and sufficient reservoir hosts spatially overlap [16,29]. The northeastern forest zone of the Greater Khingan Mountains is predominantly classified as high-occurrence risk with favorable climate and tick habitats. Nevertheless, the relatively simple host community structure and semi-closed mountainous ecological pattern restrict the large-scale proliferation of *Borrelia* in local areas, forming scattered moderate-risk patches within the extensive high-risk matrix [41,42]. The Gobi Desert in western Alxa lacks essential environmental conditions for pathogen persistence, corresponding to persistently low occurrence risk [29]. Classified by the Jenks natural breaks method [50], contiguous high-occurrence-risk belts are concentrated in the central and eastern steppes, surrounded by transitional moderate-risk buffer zones, whereas marginal desert areas represent stable low-occurrence-risk regions.

Unlike static natural occurrence risk, this study adopted AHP to quantify transmission risk by incorporating anthropogenic factors such as road networks and livestock trade, and assessed the potential for cross-regional pathogen spread [51–53]. The overall spatial pattern of transmission risk generally matched the suitability for pathogen occurrence, yet high transmission risk formed more aggregated, ribbon-shaped risk clusters across south-central Inner Mongolia. This zone constitutes a key corridor for pastoral transporta-

tion and livestock trading, where frequent human and animal movement increases the likelihood of pathogen spillover and secondary outbreaks [16]. Contrary to the natural isolation pattern reflected by occurrence risk, parts of the northeastern Greater Khingan Mountains forest exhibited elevated transmission risk driven by human travel and livestock movement between forest and grassland habitats. In contrast, sparsely populated desert areas in western Inner Mongolia showed low transmission risk. This multi-factor analytical framework distinguishes disease hotspots shaped by natural conditions from diffusion corridors driven by human activities, providing practical support for livestock quarantine and cross-jurisdictional joint prevention and control—a dimension frequently overlooked in previous regional risk assessments of tick-borne diseases.

Spatial overlay analysis was performed on the classified occurrence risk layer and transmission risk layer to generate a nine-class integrated risk zoning map, which characterizes Lyme disease hazards across Inner Mongolia under the combined effects of climate, tick vectors, reservoir hosts, and anthropogenic disturbance [52,53]. High-occurrence–high-transmission and high-occurrence–moderate-transmission integrated risk zones dominated the landscape of most of Hulunbuir and western Hinggan League. Ribbon-like high-risk areas extended across south-central Xilingol, while scattered high-risk patches were distributed in northern Bayannur, eastern Ordos, and the southern mountainous areas of Baotou. These regions feature microclimates conducive to Borrelia persistence, abundant tick and host resources, and accessible transportation networks, making them priority areas for long-term surveillance and targeted interventions [16,29]. Moderate-risk zones encircled high-risk cores in a ring pattern and acted as transitional buffer zones for disease spillover. Mixed patches of low-occurrence–moderate-transmission and low-occurrence–high-transmission risk were scattered across the central transitional steppe, indicating mismatches between natural suitability and human-mediated diffusion potential and unstable epidemic risk in these areas. The extensive desert–Gobi terrain of western Alxa formed a continuous low-occurrence–low-transmission zone, where both natural pathogen colonization and human-assisted spread were markedly constrained. This two-dimensional risk assessment framework fully accounts for the unique long-distance nomadic grazing practices in Inner Mongolia and offers spatial evidence for deploying tick surveillance sites and developing stratified Lyme disease prevention and control strategies.

4.4. Limitations

Several limitations should be noted for this study and warrant further investigation. First, uncertainty exists regarding the vector competence of the four tick species included in the model. Only *Ixodes persulcatus* has been confirmed as a competent vector of Lyme disease spirochetes in northern China, while *D. nuttalli*, *Hae. concinna* and *Hy. asiaticum* were treated merely as potential candidate vectors. Whether these three species can sustain pathogen transstadial transmission and drive spillover remains to be verified by additional laboratory and field evidence. Second, the occurrence datasets used for modeling still carry residual sampling bias. Although spatial thinning was performed to reduce clustering effects from field surveys, uneven sampling effort may distort spatial predictions. Third, our modeling framework relied mainly on broad-scale climate, vegetation, and topographic datasets, without incorporating fine-resolution variables including refined land-use categories and grazing intensity. Incorporation of field-collected host survey data in future work is expected to improve the spatial precision of risk maps. Fourth, future projections were generated using two CMIP6 GCMs (BCC-CSM2-MR, EC-Earth3-Veg) across four SSP scenarios. Climate projections nonetheless contain inherent structural uncertainty associated with model parameterization and emission assumptions.

Notably, the modeled risk layers reflect the ecological circulation potential of Lyme disease spirochetes shaped by climate, tick vectors, and host distribution, and they cannot be equated to human infection risk. Furthermore, all Lyme disease spirochete records were pooled without genospecies differentiation. Future work with genospecies-resolved data may build separate models to compare their suitable habitats. Finally, we lack independent epidemiological data for external validation. Long-term human surveillance and field *Borrelia* testing of ticks may help calibrate risk thresholds and improve the public health utility of this model.

Supplementary Materials: The following supporting information can be downloaded at: https://www.mdpi.com/article/10.3390/tropicalmed11120343/s1, Table S1: Location information of the Lyme disease spirochete detection; Table S2: Description of 29 potential influencing factors included in model development; Figure S1: Flowchart for risk analysis of Lyme disease spirochete occurrence; Figure S2: Flowchart for risk analysis of Lyme disease spirochete transmission; Table S3: AHP assessment system of Rickettsiae transmission risk; Table S4: AHP pairwise comparison matrix (A-B); Table S5: AHP pairwise comparison matrix (B1-C). Figure S3. 2050S Distribution Pattern of Lyme disease spirochete.

Author Contributions: Conceptualization, D.L. and G.; methodology, D.L. and G.; software, D.L. and Y.W. (Yu Wang); formal analysis, D.L. and G.; investigation, D.L., Y.Z., J.Z., X.L., Y.W. (Yingjie Wang), H.L., R.Z. and X.W.; resources, H.W., T., R.L., W. and G.; data curation, J.Y., Y.Z., J.Z. and X.L.; writing—original draft, D.L., J.Y. and G.; writing—review and editing, D.L., J.Y. and G.; supervision, W. and G.; project administration, W. and G.; funding acquisition, W. and G. All authors have read and agreed to the published version of the manuscript.

Funding: This work was supported by the National Natural Science Foundation of China [grant number 32360051], the Construction Program of Key Laboratory of Inner Mongolia [grant number 2025KYPT0045], and the Inner Mongolia Science and Technology Program Project [grant number 2026YFSH0038].

Institutional Review Board Statement: Tick samples were collected from the body surfaces of cattle, sheep, horses, and camels, as well as from questing ticks in wild habitats. Prior to sampling, verbal agreement was reached with livestock owners regarding the sampling purpose, procedures, and precautions, and their informed consent was obtained. The entire sampling process strictly abided by the relevant requirements of the National Guidelines for Experimental Animal Welfare of China (2006-398) to ensure that the sampling operations complied with animal welfare standards. The overall protocol of this study has been reviewed and approved by the Animal Experimental Ethics Committee of the Medical Department, Hetao College, and has been registered in accordance with the Measures for the Review of Animal Experimental Ethics of Hetao College, with the ethical registration number HTXY-YXX-2023-003 (Approval Date: 2023-03-19).

Informed Consent Statement: Not applicable.

Data Availability Statement: The original contributions presented in the study are included in the article/Supplementary Material. Further inquiries can be directed to the corresponding authors.

Acknowledgments: We gratefully acknowledge the data resources offered by the National Earth System Science Data Center (National Science & Technology Infrastructure of China, http://www.geodata.cn), the Resource and Environmental Science Data Platform (http://www.resdc.cn/), the Food and Agriculture Organization of the United Nations (https://www.fao.org/faolex/zh/) (accessed on 20 November 2024), WorldClim (https://www.worldclim.org), and the Amap Open-Platform (https://lbs.amap.com).

Conflicts of Interest: The authors declare that the research was conducted in the absence of any commercial or financial relationships that could be construed as a potential conflict of interest.

References

1. Trevisan, G.; Cinco, M.; Trevisini, S.; di Meo, N.; Chersi, K.; Ruscio, M.; Forgione, P.; Bonin, S. Borreliae Part 1: Borrelia Lyme Group and Echidna-Reptile Group. *Biology* **2021**, *10*, 1036. [CrossRef] [PubMed]
2. Radolf, J.D.; Strle, K.; Lemieux, J.E.; Strle, F. Lyme Disease in Humans. *Curr. Issues Mol. Biol.* **2021**, *42*, 333–384. [CrossRef] [PubMed]
3. Burgdorfer, W.; Barbour, A.G.; Hayes, S.F.; Benach, J.L.; Grunwaldt, E.; Davis, J.P. Lyme disease—A tick-borne spirochetosis? *Science* **1982**, *216*, 1317–1319. [CrossRef] [PubMed]
4. Marques, A.R.; Strle, F.; Wormser, G.P. Comparison of Lyme Disease in the United States and Europe. *Emerg. Infect. Dis.* **2021**, *27*, 2017–2024. [CrossRef] [PubMed]
5. Hansford, K.M.; Wheeler, B.W.; Tschirren, B.; Medlock, J.M. Questing Ixodes ricinus ticks and Borrelia spp. in urban green space across Europe: A review. *Zoonoses Public Health* **2022**, *69*, 153–166. [CrossRef] [PubMed]
6. Rollins, R.E.; Sato, K.; Nakao, M.; Tawfeeq, M.T.; Herrera-Mesías, F.; Pereira, R.J.; Kovalev, S.; Margos, G.; Fingerle, V.; Kawabata, H.; et al. Out of Asia? Expansion of Eurasian Lyme borreliosis causing genospecies display unique evolutionary trajectories. *Mol. Ecol.* **2023**, *32*, 786–799. [CrossRef] [PubMed]
7. Ai, C.X.; Wen, Y.X.; Zhang, Y.G.; Wang, S.S.; Qiu, G.C.; Shi, Z.X.; Chen, Z.Q.; Li, D.Y.; Liu, X.D. Epidemiological investigation of Lyme disease in forest areas of Hailin County, Heilongjiang Province. *Chin. J. Public Health* **1987**, *6*, 82–85. (In Chinese)
8. Hao, Q. Epidemic situation and control measures of Lyme disease in China. *Chin. J. Vector Biol. Control* **2020**, *31*, 639–642. (In Chinese)
9. Stark, J.; Li, X.; Zhang, J.; Burn, L.; Valluri, S.R.; Liang, J.; Pan, K.; Fletcher, M.A.; Simon, R.; Jodar, L.; et al. Systematic Review and Meta-analysis of Lyme Disease Data and Seropositivity for Borrelia burgdorferi, China, 2005–2020. *Emerg. Infect. Dis.* **2022**, *28*, 2389–2397. [CrossRef] [PubMed]
10. Hao, Q.; Hou, X.; Geng, Z.; Wan, K. Distribution of Borrelia burgdorferi sensu lato in China. *J. Clin. Microbiol.* **2011**, *49*, 647–650. [CrossRef] [PubMed]
11. Stanek, G.; Wormser, G.P.; Gray, J.; Strle, F. Lyme borreliosis. *Lancet* **2012**, *379*, 461–473. [CrossRef] [PubMed]
12. Steere, A.C.; Strle, F.; Wormser, G.P.; Hu, L.T.; Branda, J.A.; Hovius, J.W.R.; Li, X.; Mead, P.S. Lyme borreliosis. *Nat. Rev. Dis. Primers* **2016**, *2*, 16090. [CrossRef] [PubMed]
13. Eisen, R.J.; Eisen, L. The Blacklegged Tick, Ixodes scapularis: An Increasing Public Health Concern. *Trends Parasitol.* **2018**, *34*, 295–309. [CrossRef] [PubMed]
14. Wolcott, K.; Margos, G.; Fingerle, V.; Becker, N. Host association of Borrelia burgdorferi sensu lato: A review. *Ticks Tick. Borne Dis.* **2021**, *12*, 101766. [CrossRef] [PubMed]
15. Bergamo, S.; Trevisan, G.; Ruscio, M.; Bonin, S. Borrelia Diseases Across Eurasia. *Biology* **2025**, *14*, 1357. [CrossRef] [PubMed]
16. Liu, D.; Wulantuya; Fan, H.; Li, X.; Li, F.; Gao, T.; Yin, X.; Zhang, Z.; Cao, M.; Kawabata, H.; et al. Co-infection of tick-borne bacterial pathogens in ticks in Inner Mongolia, China. *PLoS Negl. Trop. Dis.* **2023**, *17*, e0011121. [CrossRef] [PubMed]
17. Liu, D.; Li, X.N.; Wulantuya; Fan, H.-X.; Tie, W.-F.; Ma, Y.-X.; Mei, B.-J.; Yin, X.-H.; Cao, M.-Z.; Gaowa. Free ticks and tick-borne *Borrelia* in Daxinganling forest zone, Inner Mongolia Autonomous Region, China. *Chin. J. Vector Biol. Control* **2023**, *34*, 394–399. (In Chinese)
18. Chu, C.Y.; He, J.; Wang, J.B.; Hasen, G.; Zhang, P.H.; Wu, X.M.; Zhao, Q.M.; Jiang, B.G.; Gao, Y.; Cao, W.C. Investigation on Borrelia burgdorferi sensu lato in ticks and rodents collected in Da Xing-An Mountains Forest areas of China. *Chin. J. Epidemiol.* **2006**, *27*, 681–684. (In Chinese)
19. Fang, L.Q.; Liu, K.; Li, X.L.; Liang, S.; Yang, Y.; Yao, H.W.; Sun, R.X.; Sun, Y.; Chen, W.J.; Zuo, S.Q.; et al. Emerging tick-borne infections in mainland China: An increasing public health threat. *Lancet Infect. Dis.* **2015**, *15*, 1467–1479. [CrossRef] [PubMed]
20. Wulantuya; Yin, X.H.; Cui, Y.H.; Liu, D.; Wang, T.F.; Miao, Y.R.; Amuri, H.; Cao, M.Z.; Zhao, Z.W.; Xing, F.C.; et al. Diversity and genotype analysis of tick-borne pathogens in grasslands in the central and western part of Inner Mongolia. *Chin. J. Parasitol. Parasit. Dis.* **2021**, *39*, 44–50. (In Chinese)
21. Wulantuya; Gaowa; Yin, X.H.; Cao, M.Z.; Guo, S.C.; Wang, Q.; Arbunjirgal; Liu, M.Q. Survey on Borrelia bacteria in rodents from Bayannur, Inner Mongolia Autonomous Region, China. *Chin. J. Vector Biol. Control* **2018**, *29*, 239–241. (In Chinese)
22. Lu, J.P.; Yang, X.F.; Zhao, G.; Li, Q.A.; Han, X.Z.; Tian, Y.H.; Ren, H.F.; Gong, X.W.; Zhang, J.S.; Wan, K.L.; et al. Investigation of Lyme disease in desert areas of Alxa League, Inner Mongolia. *Chin. J. Vector Biol. Control* **1996**, *3*, 188. (In Chinese)
23. Kilpatrick, A.M.; Dobson, A.D.M.; Levi, T.; Salkeld, D.J.; Swei, A.; Ginsberg, H.S.; Kjemtrup, A.; Padgett, K.A.; Jensen, P.M.; Fish, D.; et al. Lyme disease ecology in a changing world: Consensus, uncertainty and critical gaps for improving control. *Philos. Trans. R. Soc. Lond. B Biol. Sci.* **2017**, *372*, 20160117. [CrossRef] [PubMed]
24. Medlock, J.M.; Leach, S.A. Effect of climate change on vector-borne disease risk in the UK. *Lancet Infect. Dis.* **2015**, *15*, 721–730. [CrossRef] [PubMed]
25. Gray, J.S.; Dautel, H.; Estrada-Peña, A.; Kahl, O.; Lindgren, E. Effects of climate change on ticks and tick-borne diseases in Europe. *Interdiscip. Perspect. Infect. Dis.* **2009**, *2009*, 593232. [CrossRef] [PubMed]

26. Medlock, J.M.; Hansford, K.M.; Bormane, A.; Derdakova, M.; Estrada-Peña, A.; George, J.C.; Golovljova, I.; Jaenson, T.G.; Jensen, J.K.; Jensen, P.M.; et al. Driving forces for changes in geographical distribution of Ixodes ricinus ticks in Europe. *Parasit. Vectors* **2013**, *6*, 1. [CrossRef] [PubMed]
27. Mannelli, A.; Bertolotti, L.; Gern, L.; Gray, J. Ecology of Borrelia burgdorferi sensu lato in Europe: Transmission dynamics in multi-host systems, influence of molecular processes and effects of climate change. *FEMS Microbiol. Rev.* **2012**, *36*, 837–861. [CrossRef] [PubMed]
28. Diuk-Wasser, M.A.; VanAcker, M.C.; Fernandez, M.P. Impact of Land Use Changes and Habitat Fragmentation on the Eco-epidemiology of Tick-Borne Diseases. *J. Med. Entomol.* **2021**, *58*, 1546–1564. [CrossRef] [PubMed]
29. Ma, R.; Li, C.; Tian, H.; Zhang, Y.; Feng, X.; Li, J.; Hu, W. The current distribution of tick species in Inner Mongolia and inferring potential suitability areas for dominant tick species based on the MaxEnt model. *Parasit. Vectors* **2023**, *16*, 286. [CrossRef] [PubMed]
30. Takano, A.; Fujita, H.; Kadosaka, T.; Takahashi, M.; Yamauchi, T.; Ishiguro, F.; Takada, N.; Yano, Y.; Oikawa, Y.; Honda, T.; et al. Construction of a DNA database for ticks collected in Japan: Application of molecular identification based on the mitochondrial 16S rDNA gene. *Med. Entomol. Zool.* **2014**, *65*, 13–21. [CrossRef]
31. Horak, I.G.; Braack, L.E.; Fourie, L.J.; Walker, J.B. Parasites of domestic and wild animals in South Africa. XXXVIII. Ixodid ticks collected from 23 wild carnivore species. *Onderstepoort J. Vet. Res.* **2000**, *67*, 239–250. [PubMed]
32. Kawabata, H.; Dancel, L.A.; Villanueva, S.Y.; Yanagihara, Y.; Koizumi, N.; Watanabe, H. flaB-polymerase chain reaction (flaB-PCR) and its restriction fragment length polymorphism (RFLP) analysis are an efficient tool for detection and identification of Leptospira spp. *Microbiol. Immunol.* **2001**, *45*, 491–496. [CrossRef] [PubMed]
33. Graham, M.H. Confronting multicollinearity in ecological multiple regression. *Ecology* **2003**, *84*, 2609–2621. [CrossRef]
34. Dormann, C.F.; Elith, J.; Bacher, S.; Buchmann, C.; Carl, G.; Carré, G.; Marquéz, J.R.G.; Gruber, B.; Lafourcade, B.; Leitão, P.J.; et al. Collinearity: A review of methods to deal with it and a simulation study evaluating their performance. *Ecography* **2013**, *36*, 27–46. [CrossRef]
35. Radosavljevic, A.; Anderson, R.P. Making better Maxent models of species distributions: Complexity, overfitting and evaluation. *J. Biogeogr.* **2014**, *41*, 629–643. [CrossRef]
36. Muscarella, R.; Galante, P.J.; Soley-Guardia, M.; Boria, R.A.; Kass, J.M.; Uriarte, M.; Anderson, R.P. ENMeval: An R package for conducting spatially independent evaluations and estimating optimal model complexity for Maxent ecological niche models. *Methods Ecol. Evol.* **2014**, *5*, 1198–1205. [CrossRef]
37. Saaty, T.L. *The Analytic Hierarchy Process*; McGraw-Hill: New York, NY, USA, 1980; pp. 1–287.
38. Slatculescu, A.M.; Clow, K.M.; McKay, R.; Talbot, B.; Logan, J.J.; Thickstun, C.R.; Jardine, C.M.; Ogden, N.H.; Knudby, A.J.; Kulkarni, M.A. Species distribution models for the eastern blacklegged tick, Ixodes scapularis, and the Lyme disease pathogen, Borrelia burgdorferi, in Ontario, Canada. *PLoS ONE* **2020**, *15*, e0238126. [CrossRef] [PubMed]
39. Wang, X.; Shang, M.; Wang, Z.; Ji, H.; Wang, Z.; Liu, Q. Projecting the potential distribution of *Rickettsia japonica* in China and Asian adjacent regions under climate change using the Maxent model. *Front. Public Health* **2025**, *13*, 1478736. [CrossRef] [PubMed]
40. Wang, Y.; Zhang, Y.M.; Yuan, S.; Ding, Y.; Guan, X.; Gao, S.N.; Song, G.; Tang, L. Distribution of potential suitable habitats for Ixodes persulcatus in Heilongjiang Province based on the maximum entropy model. *Chin. J. Endem. Dis.* **2024**, *43*, 885–890. (In Chinese)
41. Tian, J.; Liu, J.; Zhao, H.; Chen, X.; Geng, X.; Lu, M.; Li, K. Molecular surveillance reveals a potential hotspot of tick-borne disease in Yakeshi City, Inner Mongolia. *BMC Microbiol.* **2023**, *23*, 359. [CrossRef] [PubMed]
42. Duan, L.; Zhang, L.; Hou, X.; Bao, Z.; Zeng, Y.; He, L.; Liu, Z.; Zhou, H.; Hao, Q.; Dong, A. Surveillance of tick-borne bacteria infection in ticks and forestry populations in Inner Mongolia, China. *Front. Public Health* **2024**, *12*, 1302133. [CrossRef] [PubMed]
43. Ostfeld, R.S.; Brunner, J.L. Climate change and Ixodes tick-borne diseases of humans. *Philos. Trans. R. Soc. Lond. B Biol. Sci.* **2015**, *370*, 20140051. [CrossRef] [PubMed]
44. Cunze, S.; Glock, G.; Kochmann, J.; Klimpel, S. Ticks on the move—Climate change-induced range shifts of three tick species in Europe: Current and future habitat suitability for Ixodes ricinus in comparison with Dermacentor reticulatus and Dermacentor marginatus. *Parasitol. Res.* **2022**, *121*, 2241–2252. [CrossRef] [PubMed]
45. Lemoine, M.; Cornetti, L.; Reeh, K.; Tschirren, B. Tick range expansion to higher elevations: Does Borrelia burgdorferi sensu lato facilitate the colonisation of marginal habitats? *BMC Ecol. Evol.* **2022**, *22*, 104. [CrossRef] [PubMed]
46. Georgiades, P.; Ezhova, E.; Räty, M.; Orlov, D.; Kulmala, M.; Lelieveld, J.; Malkhazova, S.; Erguler, K.; Petäjä, T. The impact of climatic factors on tick-related hospital visits and borreliosis incidence rates in European Russia. *PLoS ONE* **2022**, *17*, e0269846. [CrossRef] [PubMed]
47. McVicar, M.; Rivera, I.; Reyes, J.B. Ecology of Ixodes pacificus Ticks and Associated Pathogens in the Western United States. *Pathogens* **2022**, *11*, 89. [CrossRef] [PubMed]
48. Gui, Z.; Wu, L.; Cai, H.; Mu, L.; Yu, J.F.; Fu, S.Y.; Si, X.Y. Genetic diversity analysis of Dermacentor nuttalli within Inner Mongolia, China. *Parasit. Vectors* **2021**, *14*, 131. [CrossRef] [PubMed]

49. Estrada-Peña, A.; Ostfeld, R.S.; Peterson, A.T.; Poulin, R.; de la Fuente, J. Effects of environmental change on zoonotic disease risk: An ecological primer. *Trends Parasitol.* **2014**, *30*, 205–214. [CrossRef] [PubMed]
50. Brewer, C.A.; Pickle, L. Evaluation of methods for classifying epidemiological data on choropleth maps in series. *Ann. Assoc. Am. Geogr.* **2002**, *92*, 662–681. [CrossRef]
51. Tran, A.; Trevennec, C.; Lutwama, J.; Sserugga, J.; Gély, M.; Pittiglio, C.; Pinto, J.; Chevalier, V. Development and assessment of a geographic knowledge-based model for mapping suitable areas for rift valley fever transmission in eastern Africa. *PLoS Negl. Trop. Dis.* **2016**, *10*, e0004999. [CrossRef] [PubMed]
52. Liu, D.; Wulantuya; Wang, Y.; Zhao, J.L.; Li, X.; Lv, Z.; Luo, Y.J.; Wang, Y.; Wang, H.; Temure; et al. Ecological niche and rickettsial risk mapping of Dermacentor nuttalli in Inner Mongolia, China. *Front. Cell. Infect. Microbiol.* **2026**, *16*, 1763405. [CrossRef] [PubMed]
53. Liu, B.Y. Study on Vector Distribution, Risk Assessment and Epidemic Model of Rift Valley Fever in China. Ph.D. Thesis, Northeast Agricultural University, Harbin, China, 2020.

Disclaimer/Publisher's Note: The statements, opinions and data contained in all publications are solely those of the individual author(s) and contributor(s) and not of MDPI and/or the editor(s). MDPI and/or the editor(s) disclaim responsibility for any injury to people or property resulting from any ideas, methods, instructions or products referred to in the content.